Percolation transitions in two dimensions

Xiaomei Feng,[1,2] Youjin Deng,[3] and Henk W. J. Blöte[1,4]

[1]*Faculty of Applied Sciences, Delft University of Technology, P. O. Box 5046, 2600 GA Delft, The Netherlands*
[2]*Nanjing University of Aeronautics and Astronautics, 29 Yudao Street, 210016 Nanjing, People's Republic of China*
[3]*Physikalisches Institut, Universität Heidelberg, Philosophenweg 12, 69120 Heidelberg, Germany*
[4]*Lorentz Institute, Leiden University, P. O. Box 9506, 2300 RA Leiden, The Netherlands*

We investigate bond- and site-percolation models on several two-dimensional lattices numerically, by means of transfer-matrix calculations and Monte Carlo simulations. The lattices include the square, triangular, honeycomb kagome, and diced lattices with nearest-neighbor bonds, and the square lattice with nearest- and next-nearest-neighbor bonds. Results are presented for the bond-percolation thresholds of the kagome and diced lattices, and the site-percolation thresholds of the square, honeycomb, and diced lattices. We also include the bond- and site-percolation thresholds for the square lattice with nearest- and next-nearest-neighbor bonds. We find that corrections to scaling behave according to the second temperature dimension $X_{t2}=4$ predicted by the Coulomb gas theory and the theory of conformal invariance. In several cases there is evidence for an additional term with the same exponent, but modified by a logarithmic factor. Only for the site-percolation problem on the triangular lattice does such a logarithmic term appear to be small or absent. The amplitude of the power-law correction associated with $X_{t2}=4$ is found to be dependent on the orientation of the lattice with respect to the cylindrical geometry of the finite systems.

I. INTRODUCTION

The bond-percolation model can be described by means of the partition sum

$$Z_{\text{bond}}(p) = \prod_{\langle ij \rangle} \sum_{b_{ij}=0}^{1} [(1-p)(1-b_{ij}) + pb_{ij}] = 1, \qquad (1)$$

where the bond variables b_{ij} are located on the edges of a lattice, and labeled with the site numbers at both ends. The "bonds," i.e., the nonzero bond variables, form a network of which one may study the percolation properties. Similarly, the site-percolation problem is described by

$$Z_{\text{site}}(p) = \prod_{\langle i \rangle} \sum_{s_i=0}^{1} [(1-p)(1-s_i) + ps_i] = 1. \qquad (2)$$

In this case, the percolation problem is formed by adding bonds between all pairs (i,j) of neighboring sites that are both occupied ($s_i = s_j = 1$).

Equations (1) and (2) specify that the bonds or sites are occupied with independent probabilities p. The values of these partition sums are trivial, but the percolation properties contained in these models are not. These properties, in particular for two-dimensional models, have been investigated by a considerable number of different approaches (see [1–10] and references therein). According to the universality hypothesis, some of these properties, such as the critical exponents, are the same for different two-dimensional lattices. Other properties, such as the percolation threshold, are naturally dependent on the type of the lattice, as well as on the number of neighbors to which a given site can form a bond. If not mentioned explicitly, we consider models with bonds between nearest-neighbor sites only.

The present work reports some findings, obtained by means of Monte Carlo simulation and transfer-matrix meth-

ods. Monte Carlo simulation was used in the cases of site percolation on the diced lattice, and of bond percolation on the square lattice with nearest- and next-nearest-neighbor bonds.

The outline of this paper is as follows. In Sec. II we sketch our transfer-matrix and Monte Carlo methods. Section III describes the analyses and lists our results. The conclusions are summarized and discussed in Sec. IV.

II. NUMERICAL METHODS

Our numerical analyses employ both transfer-matrix and Monte Carlo techniques. Both approaches have their advantages. Transfer-matrix calculations yield finite-size results of high precision, typically with error margins of the order of 10^{-12}, which therefore allow the application of sensitive fitting procedures. However, the transfer-matrix results are restricted to rather small values of the finite-size parameter. In contrast, the Monte Carlo results can be applied to much larger finite sizes, but they are also subject to significant statistical errors. Which of the two techniques was applied to specific models depended on considerations of effectiveness and complexity. The site-percolation problem on the diced lattice was investigated by the Monte Carlo method, in view of the expected amount of work involved in writing the various sparse-matrix multiplication subprograms in a transfer-matrix algorithm for the diced lattice, which has inequivalent sites. While the transfer-matrix method usually yields relatively accurate results, this appeared not to be the case for the bond-percolation problem on the square lattice with crossing bonds. For this reason we also investigated this problem using the Monte Carlo method.

A. The transfer matrix

The present transfer-matrix calculations apply to models wrapped on an infinitely long cylinder, with a finite circum-

TABLE I. Some details about the transfer-matrix calculations on the various models. Transfer directions are given with respect to a set of lattice edges. Included are the largest system sizes and the linear size of the transfer matrix for that system, as well as the corresponding size of the largest sparse matrix. 8-nb square refers to the square lattice with nearest- and next-nearest-neighbor bonds.

Lattice	Type	Direction	L_{max}	Maximum size	Sparse size
Kagome	Bond	Perpendicular	13	5943200	22732740
Square	Bond	Parallel	15	87253605	87253605
Square	Bond	Diagonal	14	22732740	87253605
Triangular	Bond	Perpendicular	14	22732740	87253605
8-nb square	Bond	Parallel	10	678570	27644437
Square	Site	Parallel	16	6903561	57225573
Square	Site	Diagonal	12	26423275	125481607
Honeycomb	Site	Parallel	12	26423275	125481607
Triangular	Site	Perpendicular	17	19848489	57225573

ference L. For the bond-percolation model, which can be considered as the special case $q=1$ of the random-cluster representation of the q-state Potts model [11], we may conveniently use the numerical methods developed earlier for the random-cluster model. Our basic approach [12] is close in spirit to that of Derrida and Vannimenus [3] for the percolation model. Reference [13] describes in detail how the state of connectivity of the sites on the end row of the cylinder can be coded by means of an integer $(1,2,3,…)$ that serves as a transfer-matrix index. That work also describes the sparse-matrix decomposition of the transfer matrix. However, the various lattice structures investigated here require modifications of the sparse-matrix methods described there. In addition, the model with nearest- and next-nearest-neighbor bonds violates the condition of "well-nestedness" described in Ref. [13], so that new coding and decoding algorithms had to be devised. The transfer matrices for the site-percolation models require different modifications that, again, depend on the lattice structure. It is, in general, necessary to store the occupation number (0 or 1) of the sites on the endmost row of the lattice, as well as the state of connectivity of the occupied sites. This combined information can also be coded as an integer that plays the role of a transfer-matrix index, using the methods described in Ref. [14]. However, the state of connectedness of the occupied sites on the last row may, depending on the lattice geometry, be subject to an additional condition. If the sites on this row are nearest neighbors, such as for the square lattice with the transfer direction along one set of lattice edges, then two adjacent, occupied sites must belong to the same cluster. This reduces the number of possible connectivities. To take advantage of this reduction, the coding-decoding algorithms for the square-lattice model were modified. For the square-lattice site-percolation model with transfer in the diagonal direction, the situation is different, and the algorithms of Ref. [14] had to be used. To save memory and computer time, sparse-matrix decompositions were applied in all cases. A full description of all these algorithms is beyond the scope of this paper; we trust that it is sufficient to mention that all further relevant details are contained in or follow from the explanations given here and in Refs. [13–17].

The connectivities used here include those of the "magnetic" type, i.e., they carry information about which of the sites of the end row are connected by a percolating path to a faraway site, say on the first row of the lattice.

Using a computer with 8 gigabytes of fast memory, our algorithms can perform transfer-matrix calculations in connectivity spaces of linear dimensions up to the order of 10^8. Some details concerning the largest system sizes that could thus be handled, and the corresponding transfer-matrix sizes, appear in Table I.

The eigenvalue problem of the transfer matrix reduces in effect to separate calculations in the magnetic and nonmagnetic sectors. The calculation of the largest eigenvalue in the nonmagnetic sector trivially yields $\Lambda_0=1$. The transfer-matrix construction enables the numerical calculation of the magnetic eigenvalue Λ_1 as described earlier [13].

The analysis of these magnetic eigenvalues uses Cardy's mapping [18] which establishes an asymptotic relation between the magnetic eigenvalue and the exact magnetic scaling dimension X_h. Furthermore, we employ knowledge of the exact critical exponents from the Coulomb gas theory [6] and the theory of conformal invariance [19]. These results establish that $X_h=5/48$ for percolation models, and that the first and second thermal dimensions are equal to $X_t=5/4$ and $X_{t2}=4$, respectively.

B. Monte Carlo calculations

We employed Monte Carlo simulations for the site-percolation problem on the diced lattice, and for the bond-percolation model on the square lattice with nearest- and next-nearest-neighbor bonds. The finite systems were defined in an $L \times L$ periodic geometry, in the case of the diced lattice on the basis of a rhombus with an angle $2\pi/3$ between the main axes, as illustrated in Fig. 1. The system, including its periodic structure, displays a hexagonal symmetry. Thus, for the definition of the periodic box one has in fact the freedom to choose any two out of three main axes separated by angles $2\pi/3$. For the square lattice we employed a periodic box with the usual square symmetry, with only two main axes. A Metropolis-like procedure was applied: one visits the sites or
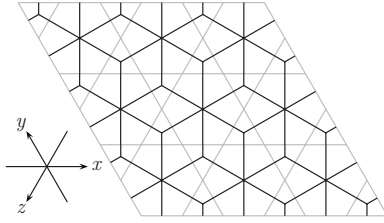
FIG. 1. Diced lattice (full lines) and its dual, the kagome lattice (thin lines). The three main axes are labeled x, y, and z.

bonds sequentially, and randomly decides with probability p whether it is occupied; clusters are then constructed on the basis of these occupied site or bond variables. We employed a random generator based on binary shift registers. To avoid errors resulting from the use of single short shift registers [20], we used the modulo-2 addition of two independent shift registers with lengths chosen as the Mersenne exponents 127 and 9689. This type of random generator is well tested [21].

For a sufficiently long series of percolation configurations thus obtained, we sampled the wrapping probability P that a configuration has *at least* one cluster that wraps across a periodic boundary and connects to itself along *any* of the aforementioned main axes. This is done for a range of values p of the site or bond probabilities.

For the analysis of the data for the model on the diced lattice, it is helpful that the value of the wrapping probability P_c is exactly known for the periodic rhombus geometry of the critical triangular bond-percolation model as $P_c = 0.683\,946\,586...$ [22] (note that $1 - \pi_+$ in the latter paper represents our P_c). It applies in the limit of large system size L and is believed to be universal, i.e., it also applies to the diced lattice, which also has a hexagonal symmetry. For the periodic square geometry, the universal value P_c is exactly known as $P_c = 0.690\,473\,725...$ [22,23].

The simulations were performed for 15 system sizes in the range $4 \leq L \leq 256$; about 21×10^9 samples were taken for each L for $L \leq 64$, and 6×10^9 samples for $L = 128$ and 256.

III. RESULTS

The analysis of the numerical finite-size data was done by means of well-documented finite-size scaling methods [24]. We describe the procedures followed for the transfer-matrix and Monte Carlo data separately.

A. Percolation thresholds

1. Transfer-matrix results

The data analysis was performed on the basis of the scaled gap

$$X_h(p,L) \equiv \frac{\zeta L \ln(\Lambda_0/\Lambda_1)}{2\pi}, \qquad (3)$$

where ζ is the geometric factor defined as the ratio between the lattice unit in which the finite size L is expressed, and the thickness of the layer added to the lattice by a transfer-matrix operation. According to finite-size scaling, the scaled gap

behaves, near the percolation threshold p_c, as

$$X_h(p,L) = X_h + a(p - p_c)L^{2-X_t} + bL^{2-X_{t2}} + \cdots, \qquad (4)$$

where a and b are model-dependent parameters. It follows from the definition of $p_c(L)$ as the solution of the equation

$$X_h(p_c(L),L) = X_h \qquad (5)$$

and from Eq. (4) that

$$p_c(L) \simeq p_c + cL^{X_t - X_{t2}} \qquad (6)$$

with $c = -b/a$. Since $X_t - X_{t2} = -11/4$, the finite-size estimates $p_c(L)$ should converge rapidly to p_c. In fact, the numerical data allow independent fitting of the exponent $X_t - X_{t2}$ and thus provide an independent confirmation of its value $-11/4$. On this basis one can, for instance, rule out a leading correction with exponent $-7/4$, such as would be generated by a hypothetical integer dimension $X = 3$. Assuming $X_{t2} = 4$, improved convergence of the X_h estimates is obtained by iterated power-law fitting as described in Ref. [13]. After a first fitting step with exponent $-11/4$, the next iteration step yielded, in most cases, an exponent with approximately the same value, which suggests that Eq. (4) should be replaced by

$$X_h(p,L) = X_h + a(p - p_c)L^{2-X_t} + (b + d \ln L)L^{2-X_{t2}} + \cdots. \qquad (7)$$

The appearance of such logarithmic terms is consistent with renormalization theory for scaling relations involving integer exponents [25]. Final estimates for the percolation threshold were obtained from another power-law iteration step. These results are shown in Table II, together with error estimates in the last decimal place.

Error estimates of the extrapolated results require considerable attention. While subsequent iteration steps eliminate successive corrections, the remaining corrections are, in principle, unknown. Fortunately, the apparent convergence of the fits indicates that they decay rapidly, i.e., with rather large and negative exponents of L. The error estimates can be based on the differences between the results from the last iteration step for a few of the largest available system sizes. The rapid decrease of these differences with increasing L suggests that the error of the extrapolated result is of the same order as the differences for the largest L values. However, it is obvious that a single estimate of this type is not very reliable, and one should search for additional evidence. First, one can vary the fitting procedure; for instance, one can fix the correction exponent at $-11/4$ in the second or the third iteration step, or treat it as a free parameter. Another variation is to use, in the second iteration step, a fit of the form given by Eq. (7). These procedures yielded consistent results, and also provide independent data on the accuracy of the extrapolations. Furthermore, the amplitude of the correction term as evaluated in the last iteration step should behave sufficiently regularly as a function of L. If not, the differences in the last iteration step are not a reliable basis for the error estimation. When these conditions were satisfied, we took the error estimate equal to a few times the typical difference between the results for the largest two systems. To

TABLE II. Summary of percolation thresholds of some two-dimensional lattices. The symbol z is the coordination number; p_c^{bond} and p_c^{site} represent the critical bond- and site-occupation probabilities, respectively. Errors in the last decimal place are given in parentheses. The value 0 is given in those cases where the percolation threshold is exactly known [2]. The remaining entries were obtained from the literature as indicated by the reference listed, or by the present numerical analyses, which use Monte Carlo simulations (as indicated by MC in the source column) or transfer-matrix calculations (as indicated by TM). The bond percolation threshold for the diced lattice follows from a duality (d) transformation of the kagome lattice model, and therefore did not require separate calculations. Similarly, the entry for the site-percolation threshold for the eight-neighbor square lattice follows from that for the matching (m) lattice, i.e., the entry for the four-neighbor model.

Lattice	z	p_c^{bond}	Source	p_c^{site}	Source
Triangular	6	0.3472964…(0)	Exact	0.5(0)	Exact
Honeycomb	3	0.6527036…(0)	Exact	0.6970402(1)	TM
				0.697043(3)	[7]
				0.69704024(4)	[26]
Kagome	4	0.52440499(2)	TM	0.6527036…(0)	Exact
		0.5244053(3)	[7]		
		0.52440503(5)	MC		
Diced	3,6	0.47559501(2)	TM,d	0.58504627(6)	MC
Square	4	0.5(0)	Exact	0.59274605(3)	TM
				0.59274603(9)	[27]
				0.59274606(5)	MC
Square	8	0.250369(3)	TM	0.40725395(3)	TM,m
		0.25036834(6)	MC		

provide some actual information about the apparent convergence of the percolation thresholds, we list the largest-L differences of the finite-size estimates of the original data, and of the first, second, and third iteration steps, for the case of the site-percolation problem on the square lattice, with transfer parallel to the edges. While these differences depend on the fit procedure, they typically amount to 2×10^{-5}, 10^{-6}, 10^{-7}, and less than 10^{-8} respectively. Furthermore, the amplitude of the last power-law step appears to tend smoothly to a constant and gives no sign of, for instance, an extremum as a function of L.

2. Monte Carlo results

The numerical results for the wrapping probability P defined in Sec. II B were fitted, using the least-squares criterion, by means of the finite-size scaling formula

$$P(p,L) = P_c + a_1(p - p_c)L^{y_t} + a_2(p - p_c)^2 L^{2y_t} + b_1 L^{y_i}$$
$$+ b_2 L^{y_i-1} + c(p - p_c)L^{y_t+y_i}, \qquad (8)$$

where $y_t = 2 - X_t = 3/4$ is the temperature exponent and $y_i = 2 - X_{t2} = -2$ is the irrelevant exponent [6] describing the corrections to scaling.

We simulated the bond-percolation model on the triangular lattice right at the exactly known critical point for 15 values of L in the range $4 \le L \le 512$. The number of samples is about 1×10^{10} for system sizes $L \le 256$, and 2×10^9 for $L=512$. The wrapping probability P was fitted by Eq. (8), excluding the p-dependent terms. We obtained $P_c = 0.683\,947(3)$, in good agreement with the exact result $0.683\,946\,586…$ [22].

For the diced lattice, the asymptotic critical wrapping probability was fixed at the exact value. The $P(p,L)$ values appear to be well described by Eq. (8) for system sizes not smaller than the minimum size $L_{\min} = 16$. Satisfactory fits (as judged from the χ^2 criterion) could also be obtained for smaller values of $L_{\min} = 16$ when additional corrections were included with exponents $y_i - 2$ and $y_i - 3$. These fits are quite stable with respect to variation of $L_{\min}$, and yield the site-percolation threshold of the diced lattice as $p_c = 0.585\,046\,27(6)$.

Also for bond percolation on the square lattice with nearest- and next-nearest-neighbor bonds we fitted the $P(p,L)$ data by Eq. (8), but with the wrapping probability fixed at $P_c = 0.690\,473\,725…$ [22,23]. Satisfactory fits were obtained for $L \ge 6$, and yield the bond-percolation threshold as $p_c = 0.250\,368\,34(6)$. The estimates for p_c are included in Table II.

The estimation of the uncertainty margin in p_c is relatively straightforward. The Monte Carlo runs are divided in 2000 subruns, and the error in the average of a run follows from the standard deviation of the subrun averages. The multivariate analysis that determines p_c thus also produces the statistical error in this quantity. However, the actual error is still subject to the effects of correction terms not included in Eq. (8).

Such additional correction terms decay rapidly with the system size, so that the finite-size cutoff parameter $L_{\min}$ is reasonably well determined by the $L_{\min}$ dependence of the residual χ^2 of the fits. This finite-size cutoff parameter naturally depends on the number of finite-size corrections included. Thus many fits were made to determine each p_c,

TABLE III. Results of the analysis of the corrections to scaling in the quantity $X_h(L)$ for a few exactly solved bond -or site-percolation models. Transfer directions are given with respect to a set of lattice edges and specify the orientation of the lattice with respect to the axis of the cylinder on which the model is wrapped. Results are shown for the amplitudes C and A of the L^{-2} and the $L^{-2} \ln L$ terms, respectively.

Lattice	Type	Direction	C	A
Square	Bond	Parallel	0.0306(1)	−0.0054(1)
Square	Bond	Diagonal	−0.0205(1)	−0.0027(1)
Triangular	Bond	Perpendicular	−0.0037(1)	−0.0036(1)
Triangular	Site	Perpendicular	0.0195(1)	0.0000(1)

varying the number of correction terms in the fit formula, and varying the minimum system size below which the finite-size data were excluded. The errors quoted are such that the margins include all one-standard-deviation lower and upper bounds of several different fits, using different fit formulas as well as a range of different acceptable values of $L_{\min}$ for each fit formula.

B. Corrections to scaling

The analysis of the finite-size data to determine the percolation thresholds in Sec. III A 1 indicated that there are corrections described by an irrelevant scaling dimension X_{t2} close to the value 4 predicted by the Coulomb gas analysis [6] and the Kac formula [28–30]. However, the analysis also suggested that corrections governed by this exponent contain a logarithmic correction factor. The models for which the percolation threshold is exactly known, such as the bond-percolation model on the square lattice and the site-percolation model on the triangular lattice, allow a study of the finite-size dependence of the scaled gap $X(p_c, L)$ at the exact critical point. In that case the corrections are due only to the irrelevant fields, and additional errors due to the uncertainty of the percolation threshold are eliminated. Analysis of the scaled gap will purportedly reveal the nature of the corrections associated with the leading irrelevant exponent. In order to focus more precisely on possible logarithmic terms, we defined the model-dependent quantity $C(L)$ as

$$C(L) \equiv (X_h(p_c, L) - X_h) L^2, \qquad (9)$$

which serves as an estimate of the amplitude of the finite-size correction term in $X_h(p_c, L)$ if a logarithmic term is absent. For a few models with exactly known percolation thresholds, we calculated finite-size data for $C(L)$ and applied a fit of the form

$$C(L) \approx C + A \ln L + B L^{-r}. \qquad (10)$$

First the parameters C and A were solved from two consecutive values of $C(L)$, with the amplitude B set to zero. The third term, which is treated as a perturbation, is then taken into account in the second step by means of an iterated power-law fit as described in Ref. [13]. This approach led to a series of apparently well-convergent estimates of the constant C and the amplitude A. These are shown in Table III.

This analysis was unable to yield good estimates of the exponent r, which indicates that there exist further correction terms, in addition to those listed in Eq. (10). However, the data were insufficient to obtain more quantitative information. The difference between the two entries for the amplitude A for the square lattice is, at least approximately, equal to 2. This factor may be attributed to the difference of a factor $\sqrt{2}$ in the length units of the finite size L for the two cases (an edge or a diagonal of the square lattice). This would suggest that the amplitude A of the logarithmic term is, unlike the amplitude C, independent of the orientation of the finite direction of the square lattice in the cylindrical geometry.

IV. CONCLUSION

We obtained numerical results for the percolation thresholds of several two-dimensional models. The results are, as far as they overlap with those in the literature, generally consistent with existing results, and the error margins are somewhat reduced. Although our result for the bond-percolation threshold of the kagome lattice model lies remarkably close to an approximate result given by Scullard and Ziff [9], the difference is quite significant, in agreement with the conclusions of these authors [9].

In our numerical analysis of the transfer-matrix data, we made use of the universality hypothesis, i.e., in all cases we assumed the validity of the exact results for the scaling dimensions of the percolation models in two dimensions [6]. However, we are able to support this assumption considerably. In addition to Eq. (4), we may use "phenomenological renormalization" [31] to determine the critical points, so that we no longer make use of prior knowledge of $X_h = 5/48$. This approach yields the same critical points, within error margins that are a few times larger than those listed in Table II. The estimates of the scaled gaps produced by the phenomenological renormalization approach match the value $5/48$ up to several decimal places, and give no sign of deviations from universality.

The analysis of the corrections to scaling is in agreement with the irrelevant scaling dimension $X_{t2} = 4$, but showed the existence of a contribution with a logarithmic factor in the transfer-matrix data for the scaled magnetic gap. The amplitude of this contribution is strongly model dependent, and possibly vanishes for the triangular site-percolation model. This raises the question in what sense the latter model could be special. It may be argued that it is the model with the highest symmetry investigated here; it has a $\pi/3$ rotational

symmetry as well as a form of self-dual symmetry because of the matching-lattice argument [2]. A corresponding logarithmic term could possibly also be present in the quantity $P(p,L)$, but we were unable to confirm its existence from our Monte Carlo data.

Furthermore, we recall that the bond-percolation model with crossing bonds (eight neighbors) lives in an extended space of connectivities because the condition of well-nestedness [13] no longer applies. Accordingly, one may postulate that these non-well-nested connectivities introduce another irrelevant field, and that additional corrections described by a new scaling dimension would appear. However, we did not find any clear sign of such new corrections.

Finally we remark that the present logarithmic terms are unrelated to those reported by Adler and Privman [32], which apply to some leading singularities. Logarithmic factors naturally appear in quantities involving the mean cluster size. The free energy of the random cluster model also serves as the generating function of percolation properties. The mean cluster size can be obtained by differentiation of the random-cluster partition sum or the free energy to the number of Potts states q. The q dependence of the critical exponents then provides a mechanism that introduces such logarithmic factors in some critical singularities.

[1] M. F. Sykes and J. W. Essam, J. Math. Phys. **5**, 1117 (1964).

[2] J. W. Essam, in *Phase Transitions and Critical Phenomena*, edited by C. Domb and J. L. Lebowitz (Academic, New York, 1983), Vol. 2.

[3] B. Derrida and J. Vannimenus, J. Phys. (France) Lett. **41**, L473 (1980).

[4] H. Kesten, Commun. Math. Phys. **74**, 41 (1980).

[5] A. Margolina, H. Nakanishi, D. Stauffer, and H. E. Stanley, J. Phys. A **17**, 1683 (1984).

[6] B. Nienhuis, in *Phase Transitions and Critical Phenomena*, edited by C. Domb and J. L. Lebowitz (Academic, New York, 1987), Vol. 11.

[7] P. N. Suding and R. M. Ziff, Phys. Rev. E **60**, 275 (1999).

[8] R. M. Ziff and P. N. Suding, J. Phys. A **30**, 5351 (1997).

[9] C. R. Scullard and R. M. Ziff, Phys. Rev. E **73**, 045102(R) (2006).

[10] Y. Deng and H. W. J. Blöte, Phys. Rev. E **72**, 016126 (2005).

[11] P. W. Kasteleyn and C. M. Fortuin, J. Phys. Soc. Jpn. **46** (Suppl.), 11 (1969); C. M. Fortuin and P. W. Kasteleyn, Physica (Amsterdam) **57**, 536 (1972).

[12] H. W. J. Blöte, M. P. Nightingale, and B. Derrida, J. Phys. A **14**, L45 (1981).

[13] H. W. J. Blöte and M. P. Nightingale, Physica A **112**, 405 (1982).

[14] X.-F. Qian, Y. Deng, and H. W. J. Blöte, Phys. Rev. E **72**, 056132 (2005).

[15] H. W. J. Blöte, F. Y. Wu, and X. N. Wu, Int. J. Mod. Phys. B **4**, 619 (1990).

[16] Y. M. M. Knops, H. W. J. Blöte, and B. Nienhuis, J. Phys. A **26**, 495 (1993).

[17] H. W. J. Blöte and M. P. Nightingale, Phys. Rev. B **47**, 15046 (1993).

[18] J. L. Cardy, J. Phys. A **17**, L385 (1984).

[19] J. L. Cardy, in *Phase Transitions and Critical Phenomena* (Ref. [6]).

[20] A. Hoogland, J. Spaa, B. Selman, and A. Compagner, J. Comput. Phys. **51**, 250 (1983); A. Hoogland, A. Compagner, and H. W. J. Blöte, in *Architecture and Performance of Specialized Computers*, edited by B. Alder, Computational Techniques Vol. 5 (Academic, New York, 1988), Chap. 7.

[21] L. N. Shchur and H. W. J. Blöte, Phys. Rev. E **55**, R4905 (1997).

[22] R. M. Ziff, C. D. Lorentz, and P. Kleban, Physica A **266**, 17 (1999).

[23] H. T. Pinson, J. Stat. Phys. **75**, 1167 (1994).

[24] For reviews, see, e.g., M. P. Nightingale, in *Finite-Size Scaling and Numerical Simulation of Statistical Systems*, edited by V. Privman (World Scientific, Singapore, 1990); M. N. Barber, in *Phase Transitions and Critical Phenomena*, edited by C. Domb and J. L. Lebowitz (Academic, New York, 1983), Vol. 8.

[25] F. J. Wegner, in *Phase Transitions and Critical Phenomena*, edited by C. Domb and M. S. Green (Academic, New York, 1976), Vol. 6.

[26] W. Zhang and Y. Deng (unpublished).

[27] M. J. Lee, Phys. Rev. E **76**, 027702 (2007).

[28] A. A. Belavin, A. M. Polyakov, and A. B. Zamolodchikov, J. Stat. Phys. **34**, 763 (1984).

[29] D. Friedan, Z. Qiu, and S. Shenker, Phys. Rev. Lett. **52**, 1575 (1984).

[30] V. G. Kac, in *Group Theoretical Methods in Physics*, edited by W. Beiglbock and A. Bohm, Lecture Notes in Physics Vol. 94 (Springer, New York, 1979), p. 441.

[31] M. P. Nightingale, Proc. K. Ned. Akad. Wet., Ser. B Palaeontol., Geol., Phys., Chem. **82**, 235 (1979).

[32] J. Adler and V. Privman, J. Phys. A **14**, L463 (1981).